Powder metallurgy processing of Nb-modified near β titanium alloys prepared with elemental powders

Victor Carvalho Opini[a], João Batista Fogagnolo[a], Vicente Amigó Borrás[b], Rubens Caram[a] and Juliano Soyama[a]

[a]School of Mechanical Engineering, University of Campinas, Campinas, Brazil; [b]Department of Production and Industrial Engineering, Polytechnic University of Valencia, Valencia, Spain

ABSTRACT

Near β Ti alloys typically show high specific strength and provide a wide spectrum of mechanical properties with different heat treatments. In this work, a commercial near β Ti alloy Ti-5553 (Ti-5Al-5V-5Mo-3Cr-0.5Fe) was prepared through powder metallurgy using the blended elemental powder approach. Additionally, alloy modifications with 6 wt.% Nb (Ti- 6Nb-5Al-2.5V-5Mo-3Cr-0.5Fe) and 12 wt.% Nb (Ti-12Nb-5Al-5Mo-3Cr-0.5Fe) were investigated. Specimens were prepared by uniaxial cold compaction of blended powders at room temperature with sintering conducted at 1300°C for 2 h under Ar atmosphere. Microstructure investigation revealed reasonable homogenisation of alloying elements and colony sizes in the order of 80-100 μm with porosity below 10%. Moreover, the bending strength of as-sintered Ti-12Nb-5Al-5Mo-3Cr-0.5Fe was about 850 MPa and the micro-Vickers hardness was approximately 370 HV. The alloy modifications with Nb increased strength without loss in flexural strain

1. Introduction

Ti-5553 (Ti-5Al-5V-5Mo-3Cr) is a near β Ti alloy developed for structural aircraft applications. Typi- cally, Ti-5553 is applied to improve performance and weight reduction [1]. It has substituted high-strength steels in landing gear structures [2] due to its attractive mechanical properties of >1000 MPa in yield strength and fracture toughness of >50 MPa√m [3]. This alloy can be heat treated to achieve high strength with considerable ductility (>15% of elongation) [4]. Moreover, the process window is larger when compared to other β Ti alloys enabling hardening in thick cross sections [5].

Alloy modifications with Nb in Ti-5553 were already investigated in the forged and heat-treated conditions to improve mechanical properties [6] or increase hardenability [7]. Opini et al. [6] investigated the microstructures and mechanical properties of heat-treated Ti-5553 and Ti-12Nb-5Al-5Mo-3Cr- 0.5Fe. The authors observed that an increase in strength took place due to nonhomogeneous α phase precipitation with Nb additions. Campo et al. [7] studied the hardenability of Nb-modified Ti-5553 and reported a reduction in the β-transus temperature with the replacement of V with Nb. The Nb addition changed the decomposition kinetics of the β phase, thus an improvement in hardenability could be achieved. Additions of 6 Nb and 12 Nb to Ti-5553 and correspondingly a reduction of V content to 2.5 V and 0 V were planned based on the Mo equival- ent criterion and resulted in similar Bo (bond order) and Md (metal d-orbital energy level) as the original alloy [6,7].

The typical processing route for Ti-5553 involves vacuum remelting and forging followed by extensive machining operations. Consequently, one of the difficulties with high-strength Ti alloys including Ti- 5553 is related to their high production costs. In this context, powder metallurgy processing offers several advantages such as fine microstructures, free of segregation, as well as enabling near-net shaping, which could save processing costs by reducing the number of secondary operations and decreasing the waste of materials. Moreover, considering the difficulties of achieving pre-alloyed powders of these complex alloys, the blended elemental powder approach is more beneficial for cost-oriented industrial processes. Powder metallurgy processing creates unique microstructures with porosity and local metastable heterogeneities that directly affect the mechanical properties. The feasibility of producing Ti-5553 has been reported with various powder metallurgy techniques including hot pressing [8,9], powder extrusion [10], conventional [11] and microwave sintering [12]. However, no systematic study on the substitution of V for Nb in Ti-5553 in powder metallurgy specimens has been conducted up to now. The blended elemental powder approach is a versatile and inexpensive method to prepare alloys even containing several alloying elements. One of the greatest difficulties is related to microstructural homogeneity and sinterability [13]. Consequently, establishing a compromise between microstructural features originated by a specific powder processing route and the resulting mechanical properties is paramount.

Therefore, the objective of this work was to investigate the replacement of V with Nb using elemental powders and its effect on the sintering behaviour and mechanical properties compared to the reference alloy Ti-5553. Specimens were prepared by cold press- ing a mixture of blended elemental powders followed by sintering under Ar atmosphere. Mechanical characterisation included micro-Vickers hardness and three- point bending tests.

2. Materials and methods

The samples of the near β Ti alloys were prepared using mixtures of elemental powders (blended elemental powder approach). The selected compo- sitions were Ti-5553 (Ti-5Al-5V-5Mo-3Cr-0.5Fe, in wt.%) and similar alloys with different Nb additions of 6 wt.% (Ti-6Nb-5Al-2.5V-5Mo-3Cr-0.5Fe) and 12 wt.% Nb (Ti-12Nb-5Al-5Mo-3Cr-0.5Fe), which will be referred to as Ti-6Nb and Ti-12Nb hereafter. The Nb additions were planned with a reduction in V con- tent to maintain the Mo equivalent, according to the study of Campo et al. [7].

As starting materials, high purity elemental pow- ders (Ti, Al, V, Mo, Cr, Nb and Fe) with slightly differ- ent particle sizes were used, Table 1. The oxygen content of the Ti and Mo powders was in the order of 1000 ppm, whereas the Nb powder was 2000ppm, according to the manufacturer (Goodfellow and Alfa Aesar, respectively). The morphology of the powders was either spherical or nearly spherical.

The powders were mixed with 0.5 wt.% paraffin (lubricant) and homogenised using a tumble mixer for 20 min. Specimens were prepared by uniaxial pressing with a 30-ton hydraulic press in a rectangular bar geometry of 30 × 13 × 5 mm^3 with approximately 750 MPa. Sintering was conducted in a tube furnace under Ar atmosphere. The heating rate was 5°C/min and an isotherm at 750°C was applied for 2 h to remove the lubricant. Sintering was carried out at a temperature of 1300°C for 2 h. After sintering, the specimens were furnace cooled to room temperature. For microstructural investigation, specimens were embedded in resin, ground and polished to 1 μm finish using diamond paste. Porosity measurements were conducted with images recorded using a light optical microscope (LOM) from Nikon, model Eclipse LV100 and with the software ImageJ. At least eight images of 100× magnifications were used for each alloy. Etching was achieved by immersion in Kroll sol- ution for 5 s. Scanning Electron Microscopy (SEM) was carried out with an EVO MA15 from Zeiss coupled with an EDS system from Oxford. Density was measured by Archimedes using a four-digit scale [14] and the theoretical density was calculated based on the weight fractions of the alloying elements. The densification was obtained through the ratio between Archimedes and the theoretical density. The characterisation of mechanical properties was carried out by micro-Vickers hardness and three-point bending tests. Micro-Vickers hardness measurements were conducted in a Buehler 2100 using a 980 mN load (HV 0.1) for 10 s. Bending tests were carried out using a universal testing machine MTS 810 at a loading rate of 0.5 mm/min and a load cell of 100 kN.

Table 1. Description of particle size and purity of metal powders.

Element	Size	Purity (%)
Ti	Maximum 45 μm	99.5
Al	Average < 45 μm	99.5
V	Maximum 45 μm	99.7
Mo	Average < 88 μm	99.5
Cr	Maximum 45 μm	99.9
Nb	Average < 45 μm	99.8
Fe	Average < 20 μm	99.8

3. Results and discussion

3.1. Sintering behaviour

The porosity of sintered specimens measured by image analysis and the densification (percentage of the theoretical density) calculated from the Archimedes density are shown in Figure 1. The reference alloy Ti-5553 showed the lowest porosity in the order of 6%, whereas with additions of Nb, the porosity increased to about 7%. Despite the change in densification, porosity values below 10% could be achieved in all cases, which indicates the presence of closed pores that are not interconnected to the surface. The difference between porosity and densification took place due to the measurement technique applied in each case. Since porosity was estimated by image analysis, it considered only a cross section of the material, whereas densification was measured by Archimedes' principle that typically provides an average of the bulk material. Regardless of the measurement method, the modifications with Nb decreased the densification because Nb is a slower diffusing element than V in Ti at the sintering temperature applied, which hindered diffusion. Consequently, by substituting V with Nb, the sinterability was inferior. Nonetheless, the same level of densification was reported by Zhao et al. [8] and Zygula et al. [11] for Ti-5553 prepared with blended elemental powders.

Sintering with blended elemental powders typically leads to lower densifications and microstructural heterogeneities due to lack of diffusion [15], especially when slow diffusing elements are present such as Nb and Mo. Nevertheless, since the densification was above 20%, the as-sintered condition could be considered adequate for less critical load-bearing components. According to L. Bolzoni et al. [16], vacuum sintering of pre-alloyed steel powder (4140) containing Cr, Mn and Mo mixed with pure hydride-dehydride Ti powder led to densifications of 80%. This level of densification resulted in comparable strength with wrought counterparts.

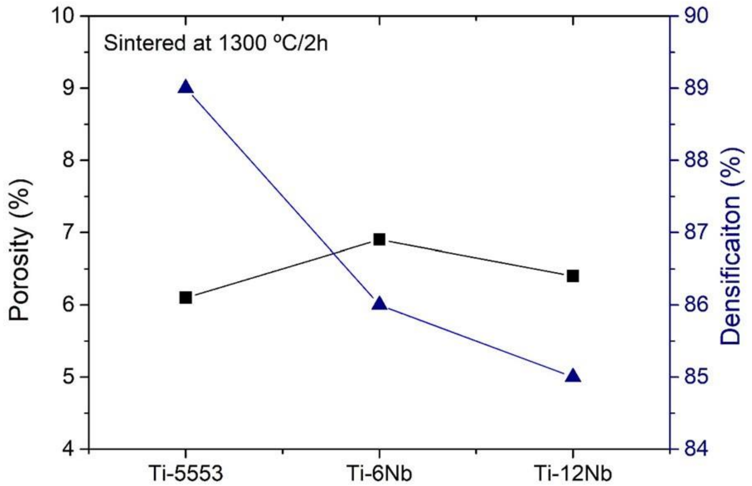

Figure 1. Porosity (black squares) and densification (blue triangles) for the different investigated alloys.

1.1. Sintered microstructures

Figure 2 shows the microstructures of sintered specimens. In all cases, it was possible to identify pores as dark and mostly round features, and grains of β phase with precipitation of α phase at grain boundaries and inside the grains. The α phase inside the grains grew with an acicular or lath-like shape. The formation of the α phase took place during cooling from the sintering temperature (1300°C) that was higher than the β-transus (850–860°C) [7,17]. After sintering, the specimens were furnace cooled, which allowed the precipitation of the α phase. The grain size was about 80–100 μm in all cases. The thickness of the α phase inside the grains decreased with Nb additions. According to Campo et al. [7], the substitution of V by Nb makes the decomposition kinetics of the β phase sluggish. Consequently, under the same cooling rate, specimens with more Nb presented a more refined α phase.

Overall the microstructures achieved were fairly homogeneous but due to the presence of slow diffusing elements, some local areas with a higher concentration of alloying elements were identified. Figure 3 shows regions of Mo heterogeneities in a Ti-12Nb alloy. The heterogeneous areas were composed of round Mo particles with a diluted interface indicating that sintering at 1300°C for 2 h was not sufficient for a complete homogenisation. Higher temperatures or longer sintering times would lead to a larger beta grain size, which is commonly associated with lower mechanical properties, especially lower ductility [18].

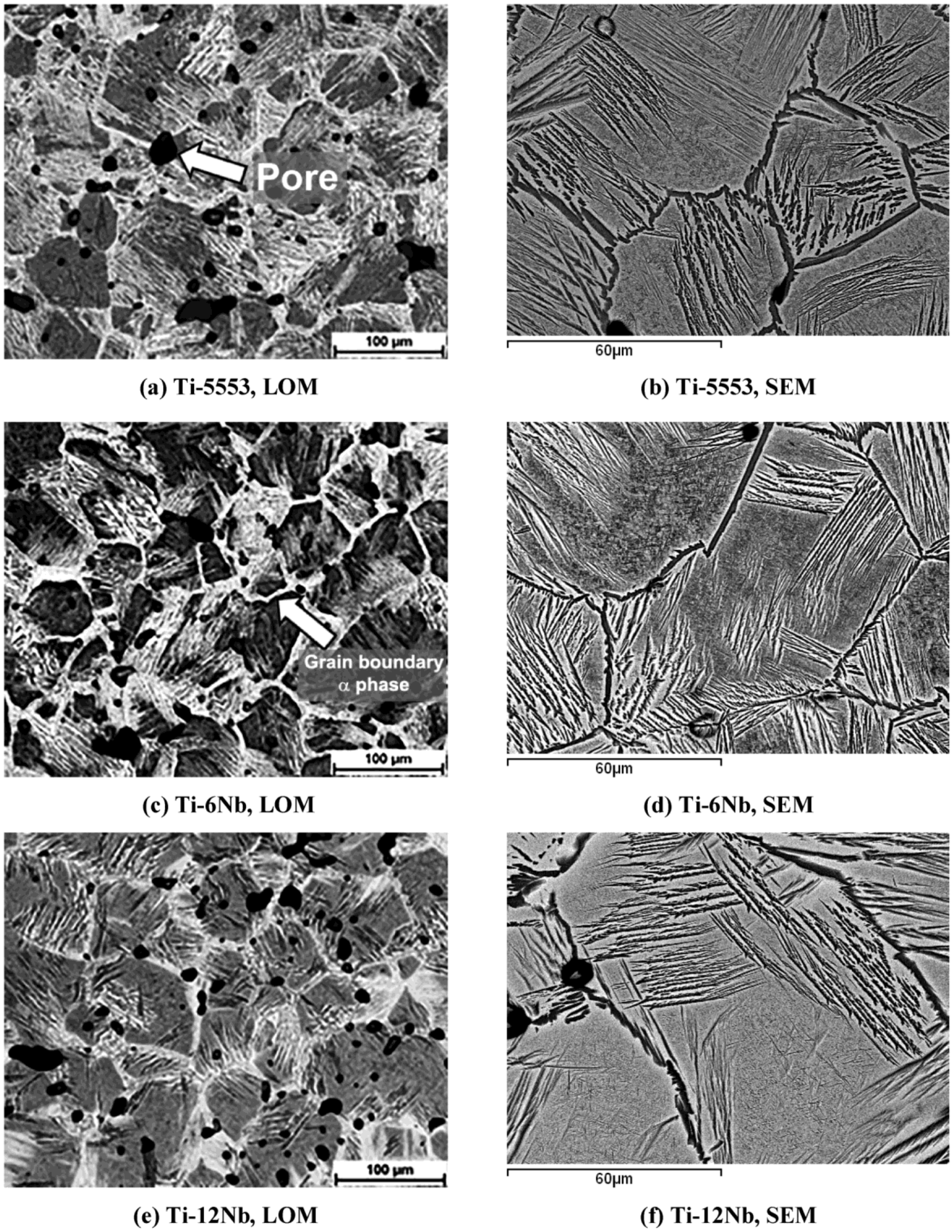

Figure 2. Sintered microstructures of investigated near β Ti alloys. (a), (c) and (d) were recorded with an optical microscope and (b), (d) and (e) with a scanning electron microscope. All images show β grains, pores and α phase precipitated at the grain boundaries and inside the grains. (a) Ti-5553, LOM. (b) Ti-5553, SEM. (c) Ti-6Nb, LOM. (d) Ti-6Nb, SEM. (e) Ti-12Nb, LOM and (f) Ti-12Nb, SEM.

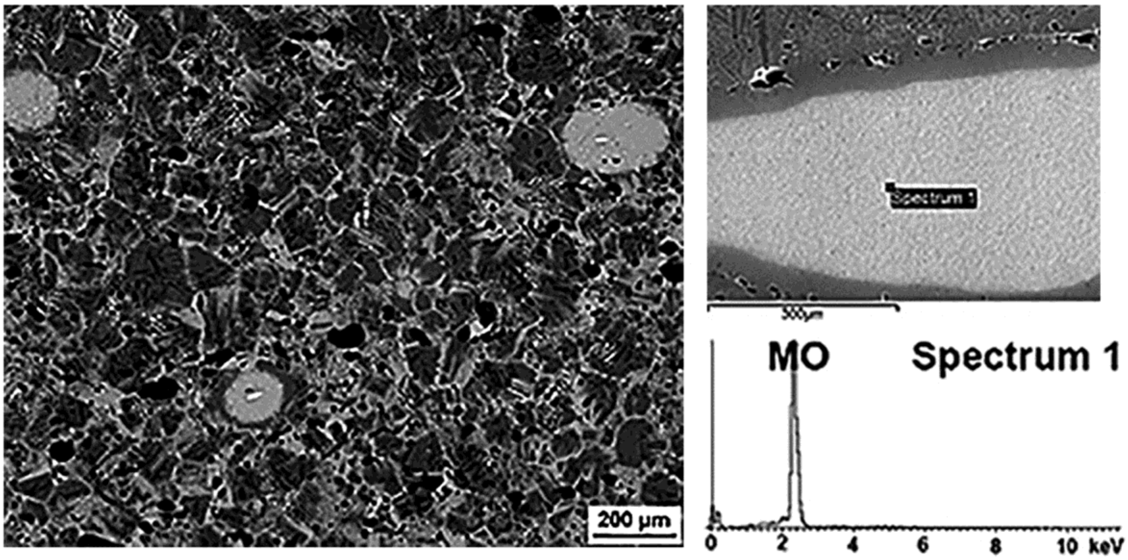

Figure 3. Micrograph showing Mo heterogeneous regions in the Ti-12Nb alloy.

1.2. *Mechanical properties*

The micro-Vickers hardness values are shown in Table 2. The average hardness was in the order of 350 HV, but the standard deviation was high in all cases. When local heterogeneities are present, e.g. porosity or lack of diffusion around slow diffusing elements, the deviation increases. The heterogeneities in the microstructure can affect the size of the micro-Vickers indentation due to the presence of harder and softer regions. For instance, a pore at the subsurface can lead to a decrease in micro-Vickers hardness and since it is not visible, the material seems to be softer. Therefore, the measurements with low loads as in micro-Vickers emphasise the effect of microstructural heterogeneities. Considering that the largest standard deviation (49 $HV_{0.1}$) was only about 13% of the average value 372 $HV_{0.1}$ in the case of Ti-12 Nb, it is possible to conclude that the effect of local heterogeneities was small. More- over, the average micro-Vickers hardness is in accordance with the study by Campo et al. [7] which reported values around 400 HV for forged Ti-5553 and Ti-12Nb that were furnace cooled.

The bending strength and fexural strain are shown in Figure 4. Despite the large standard deviation in the experimental data, there was a trend of increasing strength with the Nb content, Figure 4 (a). The reference alloy Ti-5553 showed an average of about 500 MPa, whereas Ti-12Nb reached approximately 850 MPa, which accounts for an increase of about 70%. Moreover, the flexural strain, Figure 4(b), practically remained constant with Nb additions.

Table 2. Micro-Vickers hardness of the investigated alloys.

Sintering parameters	Alloy	Micro-Vickers hardness (HV0.1/20s)
1300°C/2 h	Ti-5553	377 ± 30
	Ti-6Nb	352 ± 35
	Ti-12Nb	372 ± 48

The sintered microstructures were developed by furnace cooling from the sintering temperature of 1300°C. Since this cooling rate allowed precipitation of the α phase from the parent β phase, the α laths grew to different sizes in the investigated alloys because the precipitation kinetics was modified by the substitution of V with Nb, according to Figure 2. Nb additions induced a more sluggish β→α trans- formation, which in turn allowed Ti-6Nb and Ti-12Nb the precipitation of finer α phase at the same cooling rate. The increase in strength with the substitution of V by Nb could thus be attributed to the precipitation of finer α phase and the effect of solid solution in the β phase, considering that Nb is a larger element than V, the distortion in the crystal lattice should be larger. Moreover, the ductility of these alloys is dependent on the homogeneous deformation of the β grains, which is affected mainly by the grain size and the presence of hardening precipitates. The α phase is believed to give a more significant contribution to hardening than to plastic deformation. Therefore, considering that a finer α phase was present in sintered Ti-12Nb and a similar β grain size in comparison to the reference alloy (Ti-5553) was achieved, the strength increased and a small gain in ductility took place. The coarser α phase in sintered Ti-5553 contributed to a lower flexural strength because they can concentrate stress leading to less deformation and easing fracture through cleavage.

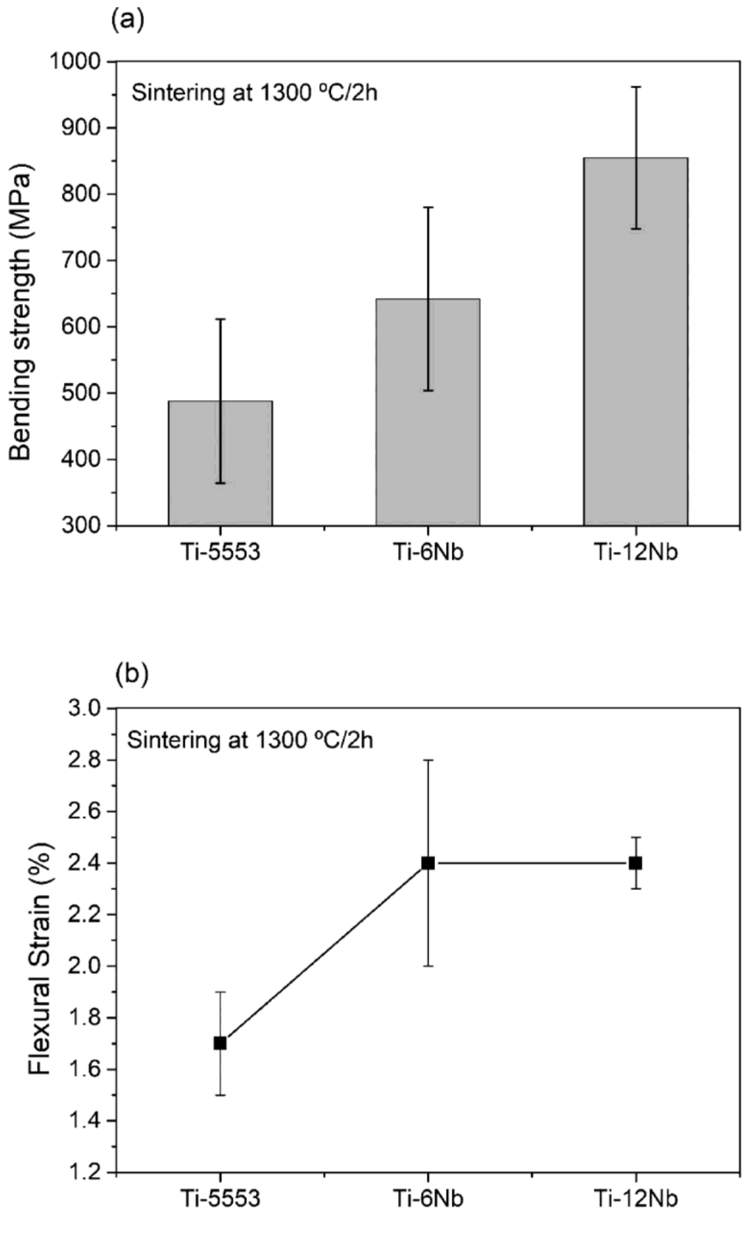

Figure 4. Bending strength (a) and flexural strain (b) of sintered near β Ti alloys.

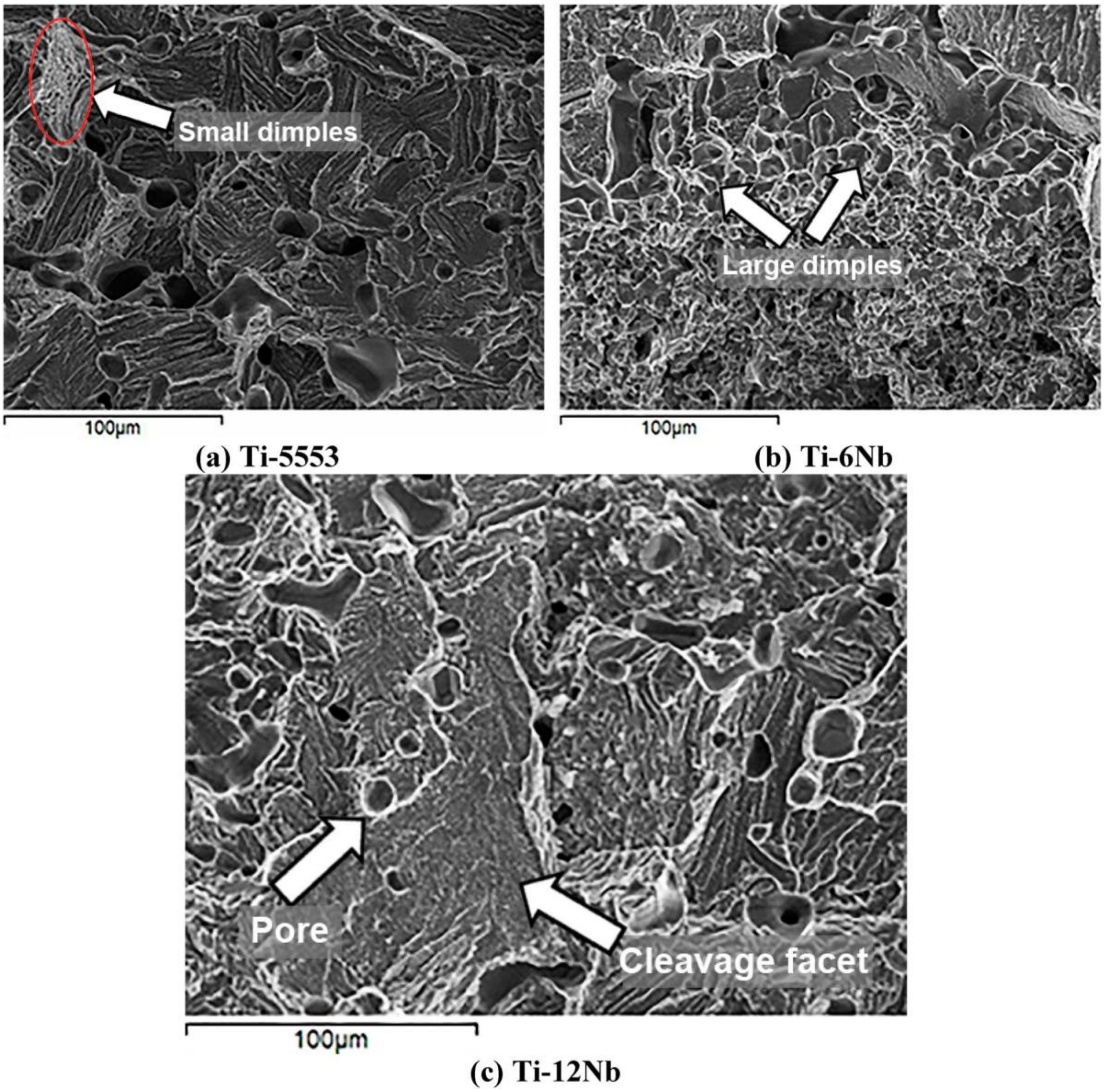

Figure 5. Fracture surfaces after the bending test. (a) Ti-5553. (b) Ti-6Nb and (c) Ti-12Nb.

1.3. *Fracture surfaces*

The fracture surfaces of sintered specimens after the bending test are shown in Figure 5. In general, the fracture was brittle as evidenced by the presence of cleavage facets with river patterns, Figure 5(a). Nevertheless, considering that a small amount of plastic deformation was measured, areas containing dimples were also observed as shown in Figure 5(a,b). The dimples varied greatly in size most likely accounting for the regions of local heterogeneities due to powder metallurgy processing. Pores could also be identified, which certainly decreased the flexural strain and toughness of the as-sintered alloys in comparison to full-dense materials. These fracture surfaces are in accordance with the work of Zhao et al. [8] that com- pared the mechanical behaviour of powder metallurgy processed Ti-5553 with specimens obtained by ingot metallurgy. The authors reported lower ductility (approximately 2.1% in tensile tests) for the powder metallurgy specimen and 3.8% for the corresponding cast counterpart.

2. Conclusions

The near β Ti alloy Ti-5553 (Ti-5Al-5V-5Mo-3Cr-0.5Fe) and its variation with Nb substituting V (Ti-6Nb-5Al-2.5V-5Mo-3Cr-0.5Fe and Ti-12Nb-5Al-5Mo-3Cr-0.5Fe) could be successfully prepared through cold pressing and conventional sintering of blended elemental powders. Despite small areas with Mo heterogeneities, the overall microstructure was homogeneous and composed of β grains with α phase precipitated during cooling from the sintering temperature. The grain size was in the order of 80- 100 μm with porosity <10%. Additions of Nb led to a systematic trend of increasing bending strength without loss in the flexural strain that could be attributed to the solid solution hardening and the change in β→α transformation kinetics, which also induced microstructural refinement.

Disclosure statement

No potential conflict of interest was reported by the author(s).

Funding

This work was supported by the São Paulo Research Foun- dation (FAPESP) under Grant 2018/18293-8, and the Brazi- lian National Council for Scientific and Technological Development (CNPq) under Grant 226462/2013-7.

References

[1] Cotton JD, Briggs RD, Boyer RR, et al. State of the art in beta titanium alloys for airframe applications. JOM. 2015;67:1281–1303. doi:10.1007/s11837-015-1442-4

[2] Boyer RR, Briggs RD. The use of β titanium alloys in the aerospace industry. J Mater Eng Perform 2013;22:2916–2920. doi:10.1007/s11665-013-0728-3

[3] Zhao Q, Sun Q, Xin S, et al. High-strength titanium alloys for aerospace engineering applications: a review on melting-forging process. Mater Sci Eng A. 2022;845:143260, doi:10.1016/J.MSEA.2022.143260

[4] Qin D, Zhao F, Li Y. The conflicts between strength and ductility of bimodal Ti-5553 alloy with fine equiaxial prior β grains. Mater Sci Eng A. 2022;841:143074, doi:10.1016/j.msea.2022.143074

[5] Kar SK, Ghosh A, Fulzele N, et al. Quantitative micro- structural characterization of a near beta Ti alloy, Ti- 5553 under different processing conditions. Mater Charact 2013;81:37–48. doi:10.1016/j.matchar.2013. 03.016

[6] Opini VC, Salvador CAF, Campo KN, et al. A phase precipitation and mechanical properties of Nb- modified Ti-5553 alloy. Mater Sci Eng A. 2016;670:112–121. doi:10.1016/j.msea.2016.06.001

[7] Campo KN, Andrade DR, Opini VC, et al. On the hardenability of Nb-modified metastable beta Ti-5553 alloy. J Alloys Compd 2016;667:211–218. doi:10.1016/j.jallcom.2016.01.142

[8] Zhao Q, Yang F, Torrens R, et al. PM versus IM Ti- 5Al-5V-5Mo-3Cr alloy in mechanical properties and fracture behaviour. Mater Res. 2019;22; doi:10.1590/ 1980-5373-MR-2018-0739

[9] Zhao Q, Yang F, Torrens R, et al. Allotropic phase transformation and high-temperature tensile defor- mation behaviour of powder metallurgy Ti-5553 alloy. Int J Refract Met Hard Mater 2020;90:105235. doi:10.1016/j.ijrmhm.2020.105235

[10] Yang F, Gabbitas B, Raynova S, et al. Preparation of Ti-5553 alloy by different extrusion processes from elemental powder mixtures. Key Eng Mater. 2018;770:31–38. doi:10.4028/www.scientific.net/ KEM.770.31

[11] Zyguła K, Wojtaszek M. The design of Ti-5Al-5Mo- 5V-3Cr elemental powders mixture processing. Arch Metall Mater 2020;65:283–289. doi:10.24425/amm. 2020.131728

[12] Raynova S, Imam MA, Yang F, et al. Hybrid micro- wave sintering of blended elemental Ti alloys. J Manuf Process 2019;39:52–57. doi:10.1016/j.jmapro. 2019.02.002

[13] Soyama J, Oehring M, Limberg W, et al. Sintering behaviour of Ti-45Al-5Nb-0.2B-0.2C

alloy modifi- cations by additions of elemental titanium and alu- minium. Powder Metall 2015;58:369–375. doi:10. 1179/1743290115Y.0000000017

[14] ASTM International. ASTM B962-17 - standard test methods for density of compacted or Sintered powder metallurgy (PM) products using Archimedes' prin- ciple. 2017 [cited 2022 Jan 26]. Available from: https://www.astm.org/b0962-17.html.

[15] Steedman G, Corbin SF, O'Flynn J. Distinguishing the influence of aluminium and vanadium additions on microstructural evolution and densification behaviour during the sintering of Ti6Al, Ti4V and Ti6Al4V. Powder Metall 2018;61:301–312. doi:10.1080/ 00325899.2018.1501946

[16] Bolzoni L, Ruiz-Navas EM, Gordo E. Quantifying the properties of low-cost powder metallurgy titanium alloys. Mater Sci Eng A. 2017;687:47–53. doi:10. 1016/j.msea.2017.01.049

[17] Fanning JC. Properties of TIMETAL 555 (Ti-5Al- 5Mo-5V-3Cr-0.6Fe). J Mater Eng Perform 2005;14:788–791. doi:10.1361/105994905X75628

[18] Markovsky PE, Bondarchuk VI, Herasymchuk OM. Influence of grain size, aging conditions and tension rate on the mechanical behavior of titanium low-cost metastable beta-alloy in thermally hardened con- dition. Mater Sci Eng A. 2015;645:150–162. doi:10. 1016/j.msea.2015.08.009